Finally, comparing eq 23, 25, and 26 reveals that the equilibrium glass-transition temperature, T_r, is mainly determined by the stiffness of the polymeric chain, which is consistent with the conclusion of the GD theory. The combination of eq 25 and 15, where the first term dominates, gives

$$\Delta\bar{\alpha}T_r \simeq \frac{\epsilon_h}{kT_r}\bar{h}_r = 0.139 \qquad (27)$$

which has the form of the Simha-Boyer equation.[2,8]

V. Conclusions

We have replaced the idea of the second-order phase transformation in the Ehrenfest sense postulated by the GD theory, yet retained its successful features in our new approach to T_r. The original Flory lattice model is used as the starting point in our analysis. The "equilibrium" freezing temperature is treated as the thermodynamic anomaly at which the most stable hole configuration is reached under the cooperative constraint of linear chain molecules. The results of our calculation compare well with the molecular parameters of polymers obtained from the GD theory by many other authors. The ubiquitous nature of the glass formation has been explained by our model even for nonpolymeric systems, while the $S = 0$ theory breaks down. The spin-related Ising anomaly and the free volume originated Simha-Boyer expression are among the special cases of the present interpretation. The equilibrium theory reported here serves as the foundation from which the role of chain conformation in kinetics will be discussed in the following paper in this issue.

Registry No. PVAc, 9003-20-7; PVC, 9002-86-2; PS, 9003-53-6.

References and Notes

(1) Fox, T. G.; Flory, P. J. *J. Appl. Phys.* **1950**, *21*, 581; *J. Polym. Sci.* **1954**, *14*, 315.
(2) Simha, R.; Boyer, R. F. *J. Chem. Phys.* **1962**, *37*, 1003.
(3) Doolittle, A. K. *J. Appl. Phys.* **1951**, *22*, 1471.
(4) Simha, R.; Curro, J. G.; Robertson, R. E. *Polym. Eng. Sci.* **1984**, *24*(14), 1071.
(5) Chow, T. S. *Polym. Eng. Sci.* **1984**, *24*, 1079.
(6) Gibbs, J. H.; DiMarzio, E. A. *J. Chem. Phys.* **1958**, *28*, 373.
(7) Eisenberg, A.; Saito, S. *J. Chem. Phys.* **1966**, *45*, 1673.
(8) Moacanin, J.; Simha, R. *J. Chem. Phys.* **1966**, *45*, 964.
(9) Havlicek, I.; Vojta, V.; Ilavsky, M.; Hrouz, J. *Macromolecules* **1980**, *13*, 357.
(10) Havlicek, I.; Nicolais, L. *Polymer* **1986**, *27*, 921.
(11) Oel, H. J.; Rehage, G. *Macromolecules* **1977**, *10*, 1036.
(12) DiMarzio, E. A. *Ann. N. Y. Acad. Sci.* **1981**, *371*, 1.
(13) Volkenshtein, M. V. *Sov. Phys. Dokl.* (*Engl. Transl.*) **1959**, *4*, 351.
(14) Flory, P. J. *Proc. R. Soc. London, Ser. A* **1956**, *A234*, 60.
(15) O'Reilly, J. M.; Mosher, R. A. *J. Polym. Sci., Polym. Phys. Ed.* **1981**, *19*, 1187.
(16) Birshtein, T. M.; Ptitsyn, O. B. *Conformations of Macromolecules*; Interscience: New York, 1966; Chapter 4.
(17) Ziman, J. M. *Principles of the Theory of Solids*; Cambridge University Press: Cambridge, 1965; p 307.
(18) Chow, T. S. *J. Polym. Sci.* **1987**, *B25*, 137; *J. Rheol.* **1986**, *30*(4), 729.
(19) O'Reilly, J. M. *J. Appl. Phys.* **1977**, *48*, 4043.
(20) Bestul, A. B. *Physics of Non-Crystalline Solids*; Prins, J. A., Ed.; North-Holland: 1965; p 426.
(21) Bucaro, J. A.; Dardy, H. D.; Corsaro, R. D. *J. Appl. Phys.* **1975**, *46*, 741.

The Role of Chain Conformation in the Theory of Glasses. 2. Enthalpy Relaxation

T. S. Chow

Xerox Corporation, Webster Research Center, 800 Phillips Road 0114-39D, Webster, New York 14580. *Received March 16, 1988; Revised Manuscript Received July 28, 1988*

ABSTRACT: We have incorporated the role of the conformational energies of polymer chains in the kinetic theory of glasses by extending the equilibrium analysis developed in the first paper of this series. Under the cooperative constraints of hole distributions, a large number of conformational energy states are also introduced for the purpose of analyzing the nonequilibrium behavior. The departures from equilibrium for holes and flex bonds are then treated as a non-Markovian stochastic process. The theory shows how the kinetics of holes and bond rotations affect the enthalpy relaxation. The calculation reveals that the conformational activation energy is between 1 and 2 orders of magntiude lower than the hole activation energy. As a result, the enthalpy relaxes much faster than the volume at short times but approaches the same relaxation rate of volume at long times.

I. Introduction

There has been considerable interest in the structure relaxation and physical aging of glass-forming systems in recent years.[1-4] Free volume has played a central role in the molecular interpretation of the glass transition and the glassy state of polymers.[5-10] The concept has been generalized quite successfully in describing the volume relaxation and recovery processes. However, in the first paper[11] (which will be denoted as 1) of this series, we have seen that free volume alone cannot provide an adequate description of the glass temperature and enthalpy behavior of polymers. The role of chain conformation must enter the physical picture in order to gain a molecular understanding of the enthalpy relaxation in polymers. There is very little theoretical development in this area.

The purpose of this paper is to incorporate the effect of chain conformation in the kinetic theory of glasses by extending the equilibrium consideration developed in 1. In our earlier studies,[10] the kinetics of free volume over the glass-transition region is found as a result of the collapse of a series of free volumes having different levels of energies of hole formation. Its mean value determines thermodynamic equilibrium and intermolecular interaction and is equal to the hole energy used in 1. The same idea will be extended to the conformational energy. The conformational kinetics will be treated as a series of relaxational processes governed by a nonequilibrium transition-state theory. Both the volume and enthalpy relaxations will be calculated and compared. The success and the limitation of the free volume concept will be discussed.

II. Internal States

As mentioned in 1, we consider a system of n holes (or free volumes) and n_x polymer molecules of x monomer

0024-9297/89/2222-0701$01.50/0

segments each. The total system consists of N sites with each site occupying a unit volume cell (v). The change in hole population with time (t) and temperature (T) determines the hole relaxation process. Following the notion of continuous conversion between holes and phonons,[5,10] we have introduced the physical picture of quantized hole energy states $\epsilon_h^{(i)}$ with $i = 1, 2, ..., L$. The problem is to determine the distribution of the ensemble characterized by a set of hole numbers with $\sum_i n_i = n$. Minimizing the excess configurational Gibbs free energy with respect to n_i, we obtain the equilibrium hole number $\bar{n}_i \sim \exp(-\epsilon_h^{(i)}/kT)$ in a clustering state i which has the form of the average number of phonons at higher phonon energies.[12] Similar to phonons, holes are created by raising the temperature and eliminated by lowering it. The ratio of $n_i/N = h_i$ is defined as the ith contribution to the free volume fraction ($h = \sum_i h_i$) with its equilibrium value[10]

$$\bar{h} = \sum_{i=1}^{L} \bar{h}_i = \bar{h}_r \exp\left[-\frac{\epsilon_h}{k}\left(\frac{1}{T} - \frac{1}{T_r}\right)\right] \quad (1)$$

where the mean energy of hole formation is $\epsilon_h = \sum_i \epsilon_h^{(i)} \bar{h}_i / \bar{h}$, k is the Boltzmann constant, and the subscripts h and r refer to the hole and the condition at $T = T_r$, respectively. The reference temperature is chosen to be the glass temperature discussed in 1. The equilibrium fraction of bonds ($\bar{f}$) for all molecules in the higher conformational energy state having the mean flex energy (ϵ_f) will also be quantized under the cooperative constraints of hole distributions. In the analysis of the nonequilibrium behavior, the system is assumed to have a set of intramolecular energy levels, 0 and $\epsilon_f^{(j)}$, with $j = 1, 2, ..., M$.[12] The partition function of the "Fermi oscillators" is

$$Q = \prod_{j=1}^{M}\left[1 + \exp\left(-\frac{\epsilon_f^{(j)} - \mu}{kT}\right)\right] \quad (2)$$

where μ is the chemical potential and the subscript f refers to the flex bond. Hence, the equilibrium fraction of the flex bonds is

$$\bar{f} = kT\frac{\partial \ln Q}{\partial \mu} = \sum_{j=1}^{M}\left[1 + \exp\left(\frac{\epsilon_f^{(j)} - \mu}{kT}\right)\right]^{-1} \equiv \sum_{j=1}^{M} \bar{f}_j = 1\Big/\left[1 + \exp\left(\frac{\epsilon_f - \mu}{kT}\right)\right] \quad (3)$$

and the mean flex (intramolecular) energy is

$$\epsilon_f = \mu + kT^2 \frac{\partial \ln (Q - 1)}{\partial T} = \sum_{j=1}^{M} \epsilon_f^{(j)} \bar{f}_j / \bar{f} \quad (4)$$

where $\bar{f}_j$ is the equilibrium bond fraction in a internal state j with the flex energy $\epsilon_f^{(j)}$. One important difference between holes and conformers (rotamers) needs to be emphasized. The number of holes is not conserved, but the number of conformers in high- and low-energy states is constant.

In the nonequilibrium case, the time derivative of the configurational entropy can be written as

$$\frac{\mathrm{d}S}{\mathrm{d}t} = \sum_{i=1}^{L}\frac{\partial S}{\partial n_i}\frac{\mathrm{d}n_i}{\mathrm{d}t} + \sum_{j=1}^{M}\frac{\partial S}{\partial f_j}\frac{\mathrm{d}f_j}{\mathrm{d}t} \simeq \frac{N}{T}\left[\sum_{i=1}^{L}\epsilon_h^{(i)}\frac{\mathrm{d}h_i}{\mathrm{d}t} + (1 - \bar{h})\sum_{j=1}^{M}\epsilon_f^{(j)}\frac{\mathrm{d}f_j}{\mathrm{d}t}\right] > 0 \quad (5)$$

which is a microscopic expression for the second law of thermodynamics. In contrast to the $S = 0$ theory,[13] the entropy production per unit time inside the system serves as the thermodynamic driving force for structure relaxation in the polymer glass.

III. Hole Kinetics

The departure from equilibrium for holes in response to molecular motion and thermal fluctuations is treated as a non-Markovian stochastic process. When all interlevel correlations are ignored, the kinetic behavior is governed by

$$\mathrm{d}n_i/\mathrm{d}t = n_x\Lambda_{xi} - n_i\Lambda_{ix} \qquad (i = 1, ..., L) \quad (6)$$

where the transition probabilities per unit time for hole creation and hole annihilation are represented by Λ_{xi} and Λ_{ix}, respectively. Equation 6 is based on the idea of continuous conversion of the number of holes and the number of phonons. When further analysis of eq 6 is carried out, the departure from equilibrium, $\delta = h - \bar{h}$, for a system started from equilibrium is[10]

$$\delta(t) = \sum_{i=1}^{L}\delta_i = -\left[\int_0^t q\sum_{i=1}^{L}\left(\frac{\partial \bar{h}_i}{\partial T}\right)_p \exp\left(-\frac{t - t'}{\tau_h^{(i)}}\right)\mathrm{d}t'\right] \quad (7)$$

where q is the cooling (<0) rate, $\tau_h^{(i)} = \tau_{hr}^{(i)}\lambda_h = \Lambda_{ix}^{-1}$ is the ith relaxation time, and the local shift factor (time scale) in the vicinity of the glass transition is

$$\lambda_h = \exp\left[-\frac{\bar{\alpha}_{hr}(T - T_r) + \delta}{\bar{h}_r^2}\right] \quad (8)$$

with $\bar{\alpha}_{hr} = (\partial\bar{h}/\partial T)_r$. In the above equation, the first term is controlled by the local activation energy $E_h = \epsilon_h/\bar{h}_r$, and the structural-dependent term $\delta/\bar{h}_r^2$ is related to the nonequilibrium entropy fluctuations in glasses.[10] In the case of isothermal annealing followed by quenching from an elevated liquid temperature T_0 to T below the glass transition, eq 7 becomes

$$\delta(t) = [\bar{h}(T_0) - \bar{h}(T)]\phi(t) \quad (9)$$

with the normalized relaxation function for holes

$$\phi(t/\tau_h) = \sum_{i=1}^{L} g_i \exp(-t/\tau_h^{(i)}) \quad (10)$$

where $g_i = \epsilon_h^{(i)}\bar{h}_i/\epsilon_h\bar{h}$ is the distribution of holes energies at a given state and is related to ϕ by a discrete Laplace transform. By letting

$$\frac{\tau_h^{(i)}}{\tau_h} = \frac{\tau_{hr}^{(i)}\lambda_h}{\tau_{hr}a_h} \rightarrow \frac{1}{u} \qquad g_i \rightarrow g(u) \quad (11)$$

the summation in eq 10 can be written as an integral

$$\phi(t/\tau_h) = \int_0^\infty g(u)e^{-ut/\tau_h}\,\mathrm{d}u \quad (12)$$

When the distribution is the δ function, $g(u) = \delta(u - 1)$, the distinction between the local and global (a_h) shift factors disappears and the relaxation function decays exponentially. Equations 11 and 12 reveal that the local and global relaxation times cannot be the same when $g(u)$ has a broader distribution and is not limited to a value at $u = 1$.

In order to understand how the local and global relaxation time scales are related, we have to discuss the motion of holes. According to eq 9, holes are frozen in a nonequilibrium state at $t = 0$ when the system is quenched from T_0 to T. During isothermal annealing, the relaxation function, $\phi(t)$, is interpreted as the holes having not reached their equilibrium states. By considering that holes diffuse on a fractal structure, the hole motion in an energy state is described by a stochastic process. The spatial-dependent master equation (eq A-2) serves as the equation of hole motion, and the motion is then expressed in terms of the mean square displacement $\langle \Delta r^2 \rangle$ (see Appendix). It is important to mention that the calculation is under the assumption of self-similar, which is a common feature for all scaling analyses.[14]

The probability of a hole in the ith energy state having reached equilibrium within a time interval t can then be written as

$$(n_i/n)(\langle \Delta r_i^2 \rangle^{1/2}/l) \tag{13}$$

Here the hole density is $n_i/n \simeq 1/L$, and $\langle \Delta r_i^2 \rangle^{1/2}/l$ is the probability for a hole traveling a distance l within the time interval t, where l is the average length (size) of an energy state. Thus, we write

$$\phi(t) = \prod_{i=1}^{L}\left(1 - \frac{n_i \langle \Delta r_i^2 \rangle^{1/2}}{nl}\right) \simeq \left(1 - \frac{\langle \Delta r^2 \rangle^{1/2}}{Ll}\right)^L \rightarrow \exp(-\langle \Delta r^2 \rangle^{1/2}/l) \quad \text{as } L \rightarrow \infty \tag{14}$$

where $\langle \Delta r^2 \rangle$ averages over holes in all states. Comparing eq 12 and 14, we obtain a basic relationship between the hole motion and the hole energy spectrum

$$\langle \Delta r^2 \rangle = l^2\left(\ln \int_0^{\infty} g(u) e^{-ut/\tau_h}\, du\right)^2 \tag{15}$$

When the hole energy spectrum is given, the motion of holes and the relaxation function are determined. In addition, we also find that $\langle \Delta r^2 \rangle$ is inversely proportional to λ_h^2 (see eq A-8 in the Appendix), which helps us in establishing the link between the local and global relaxation time scales. As a first example, $g(u)$ is chosen to be the δ function mentioned earlier, and eq 15 gives

$$\langle \Delta r^2 \rangle = (l/\tau_h)^2 t^2 \tag{16}$$

which confirms that $a_h = \lambda_h$, and $\phi = \exp(-t/\tau_h)$.

In the second case, we consider a Gaussian spectrum which has the form

$$g(u) = \frac{u^{3/2}}{2\pi^{1/2}} \exp(-u/4) \tag{17}$$

where $1/u$ is defined in eq 11 as the nondimensional hole relaxation time. Substituting eq 17 in eq 15, we obtain

$$\langle \Delta r^2 \rangle = (l^2/\tau_h)t \tag{18}$$

which gives $a_h = \lambda_h^2$, and $\phi = \exp[-(t/\tau_h)^{1/2}]$.

When $g(u)$ is non-Gaussian, eq 16 and 18 suggest that the mean square displacements should have the form

$$\langle \Delta r^2 \rangle = (l^2/\tau_h^{2\beta})t^{2\beta} \qquad 0 < \beta \leq 1 \tag{19}$$

This is consistent with Mandelbrot's notion of self-similarity in fractal structure.[15] In analyzing the equation of state and physical aging data on the basis of our hole model for relaxation in glasses, we found that $\beta = 1/2$ for most amorphous polymers[16] and it is much smaller than $1/2$ for cross-linked polymers.[17] This is due to the tenuous structure in a fractal lattice. The random motion of holes will encounter many dead ends and be forced to return. Thus, holes will need more time to travel $\langle \Delta r^2 \rangle^{1/2}$ than they would need on a Gaussian lattice. Equation 19 leads to

$$\phi(t) = \exp[-(t/\tau_{hr} a_h)^{\beta}] \qquad 0 < \beta \leq 1 \tag{20}$$

and

$$\ln a_h = \ln \lambda_h/\beta = \frac{\bar{\alpha}_{hr}(T_r - T) - \delta}{\beta \bar{h}_r^2} \tag{21}$$

IV. Conformational Kinetics

A similar approach is extended to analyze the nonequilibrium behavior of bond rotations. The governing equations are

$$\frac{df_j}{dt} = -\frac{f_j - \bar{f}_j}{\tau_f^{(j)}} \qquad (j = 1, ..., M) \tag{22}$$

Here the jth relaxation time $\tau_f^{(j)} = \tau_{fr}^{(j)}\lambda_f$ with the local shift factor

$$\lambda_f \sim \exp\left(\frac{E_f}{kT} - \frac{\delta S_f}{k}\right) \tag{23}$$

where E_f is the activation energy controlling the local rotational relaxation, and δS_f is conformer's contribution to the change of entropy related to the nonequilibrium fluctuations in glasses.[10] The Doolittle equation relates the segmental mobility to free volume.[18] By extending this idea to fv_f where v_f is the flex volume introduced in 1, the dependence of λ_f on f can then be written as

$$\ln \lambda_f = \frac{1}{\bar{f} + \theta} - \frac{1}{\bar{f}_r} \simeq \left[\left(\frac{\partial \bar{f}}{\partial T}\right)_r (T_r - T) - \theta\right] \Big/ \bar{f}_r^2 \tag{24}$$

where $\theta = f - \bar{f}$. Upon comparing eq 23 and 24 in the vicinity of the glass transition, we obtain

$$E_f = \epsilon_f(1 - \bar{f}_r)/\bar{f}_r \tag{25}$$

and

$$\delta S_f/k = \theta/\bar{f}_r^2 \tag{26}$$

Substracting both sides of eq 22 using

$$d\bar{f}_j/dt = q(\partial \bar{f}_j/\partial T)_p = q\epsilon_f^{(j)}\bar{f}_j(1 - \bar{f}_j)/kT^2 \tag{27}$$

we obtain

$$d\theta_j/dt = -\theta_j/\tau_f^{(j)} - q(\partial \bar{f}_j/\partial T)_p \qquad (j = 1, ..., M) \tag{28}$$

The solution of eq 28 for a system started from equilibrium is

$$\theta(t) = -\left[\int_0^t q\sum_{j=1}^{M}\left(\frac{\partial \bar{f}_j}{\partial T}\right)_p \exp\left(-\frac{t - t'}{\tau_f^{(j)}}\right) dt'\right] \tag{29}$$

If the same discussion that led to eq 19–21 is followed, the motion of rotamers is considered as a random walk of barriers to rotation on a fractal lattice and is expressed in terms of the mean square angular displacement similar to eq 19. Therefore, the normalized relaxation function for rotamers has the form

$$\psi(t) = \exp[-(t/\tau_{fr} a_f)^{\gamma}] \qquad 0 < \gamma \leq 1 \tag{30}$$

and the global shift factor (a_f) is linked to that of the local state (λ_f) by

$$\ln a_f = \ln \lambda_f/\gamma = [(\partial \bar{f}/\partial T)_r(T_r - T) - \theta]/\gamma \bar{f}_r^2 \tag{31}$$

A comparison of the hole, flex, and local activation energies is shown in Table I where the values of ϵ_h and $\bar{h}_r$ for poly(vinyl acetate) (PVAc) and eq 25 in 1 are used. It reveals that the activation energy for rotamers is between 1 and 2 orders of magnitude smaller than that of holes. Assuming a Gaussian distribution, $\gamma = 1/2$, the temperature dependence of log a_f for PVAc quenched from $T = T_r + 5$ K and annealed at different temperatures and times is shown in Figure 1. An Arrhenius-type temperature dependence with the global (macroscopic) activation energy equal to 3.88 kcal/mol is reached in 12 min as the contribution from the nonequilibrium term $\theta/\gamma\bar{f}_r^2$ in eq 31

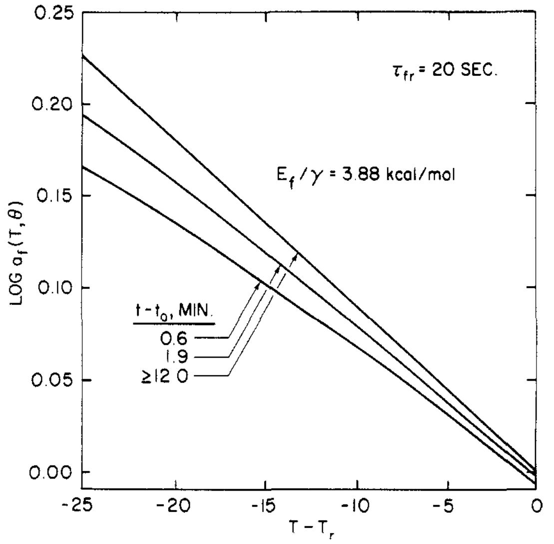

Figure 1. Shift factor a_f as a function of annealing time and temperature.

Table I
Hole, Flex, and Local Activation Energies

	hole	conformer
thermodynamic equilibrium	$\epsilon_h = 2.51$ kcal/mol	$\epsilon_f = \epsilon_h/2.16 = 1.16$ kcal/mol
ref fraction	$\bar{h}_r = 1/30$	$\bar{f}_r = 0.374$
barrier for local kinetics	$E_h = \epsilon_h/\bar{h}_r = 75.3$ kcal/mol	$E_f = \epsilon_f(1-\bar{f}_r)/\bar{f}_r = 1.94$ kcal/mol

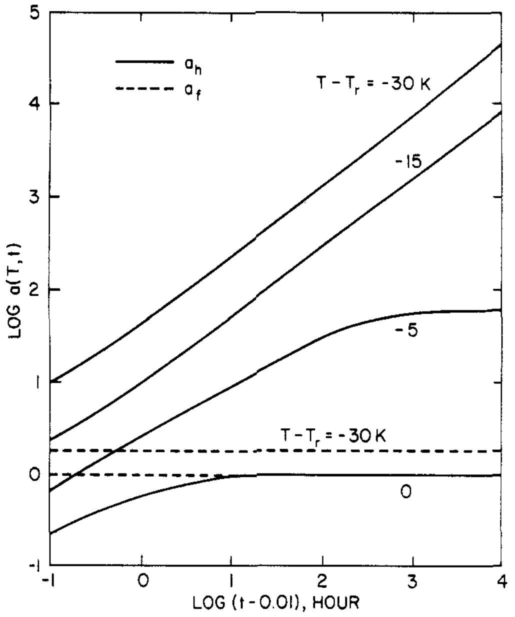

Figure 2. Effect of isothermal annealing on the shift factors a_h and a_f.

diminishes. The theoretical result is in good agreement with an experimental observation[19] that the significant conformational changes occur only in the initial stage of annealing process. Figure 2 shows that the isothermal annealing has a stronger effect on a_h rather than on a_f. For a long annealing time in the glassy state, we see a power law relationship between a_h and t. In the glass-transition region, there is no such simple relationship as illustrated by the curve at $T = T_r - 5$ in Figure 2. The nonequilibrium effect on log a_h approaches zero for $T > T_r$. Physically, this is quite similar to that for log a_f, the difference is that it takes much longer for δ to approach equilibrium.

V. Enthalpy Relaxation

The time-dependent change in the enthalpy of polymers has been studied.[20-23] There is an indication that volume and enthalpy relax differently. The conformational contribution has shown a strong effect on the equilibrium enthalpy as discussed in 1 and is included here to estimate the nonequilibrium changes. In accordance with our model, the total volume is

$$V = vN = \bar{v}\bar{N} + \bar{v}(n - \bar{n}) + v_f\bar{N}(f - \bar{f}) + \ldots \qquad (32)$$

Thus, the departure from equilibrium is

$$\frac{V - \bar{V}}{\bar{V}} = \delta(t) + \left(\frac{v_f}{\bar{v}}\right)\theta(t) \qquad (33)$$

From eq 6 in 1, the nonequilibrium configurational enthalpy is determined by

$$\frac{H - \bar{H}}{\epsilon_h\bar{N}} = \delta(t) + \left(\frac{\epsilon_f}{\epsilon_h}\right)(1 - \bar{h})\theta(t) \qquad (34)$$

Equations 33 and 34 are expressed in terms of the time-dependent hole and conformational changes. The concept of free volume has been quite successfully extended to describe volume relaxation because $v_f \ll \bar{v}$, but it becomes inadequate for enthalpy relaxation due to $\epsilon_f/\epsilon_h \simeq 1/2$. For a system starting from equilibrium, eq 34 can be written more explicitly as

$$\frac{H - \bar{H}}{\epsilon_h\bar{N}} = -\left[\int_0^t \frac{q}{kT^2}[\epsilon_h\bar{h}\phi(t - t') + (1 - \bar{h})(\epsilon_f^2/\epsilon_h)\bar{f}(1 - \bar{f})\psi(t - t')]\, dt'\right] \qquad (35)$$

where $\phi(t)$ and $\psi(t)$ are given by eq 20 and 30, respectively. In the case of quenched and annealed glasses, eq 34 becomes

$$\frac{H - \bar{H}}{\epsilon_h\bar{N}} = [\bar{h}(T_0) - \bar{h}(T)]\phi(t) + (1 - \bar{h})\left(\frac{\epsilon_f}{\epsilon_h}\right)[\bar{f}(T_0) - \bar{f}(T)]\psi(t) \qquad (36)$$

All the input parameters for holes (ϵ_h, $\bar{h}_r$, τ_{hr}, β) and rotamers (ϵ_f, $\bar{f}_r$, τ_{fr}, γ) and the relationships between them and T_r have been discussed. Upon use of these predetermined parameters for PVAc, the calculated enthalpy relaxations at different annealing temperatures are shown in Figure 3. The rapidly decreasing rate for the broken lines is due to the significantly lower conformational activation energies (local and global) shown in Table I and Figure 1. Such a rapid change in enthalpy is observed by Filisko (see p 900 of ref 3). As we have seen from eq 33 and 34, the solid curves are the approximations for the volume relaxations. The calculation reveals that enthalpy relaxes faster than volume at short times but approaches the same relaxation rate of volume at long times. This is consistent with the recent finding[22] that the activation energies controlling the effective relaxation times, which characterize the long time behavior, for volume and enthalpy are very close to each other. Finally, it is worthwhile to mention that the equilibrium number of lattice sites appearing in eq 36 is not a linear function of temperature as has often been assumed in the glassy state but is given by[16]

$$\bar{N} = \frac{\bar{N}_r \exp[2(\bar{\alpha}_{hr} + \alpha_0)(T^{3/2} - T_r^{3/2})/3T_r^{1/2}]}{1 + \alpha_0(T - T_r)} \qquad (37)$$

where α_0 is the lattice thermal expansion coefficient.

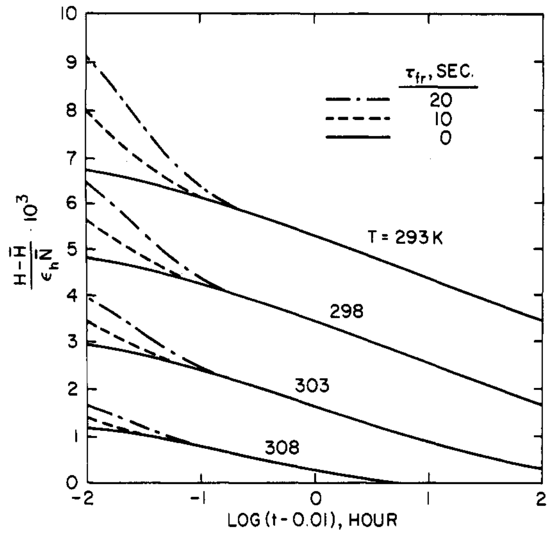

Figure 3. Comparison of the volume and enthalpy relaxations.

VI. Conclusions

Free volume provides a good basis for the molecular interpretation of volume relaxation but becomes inadequate for enthalpy relaxation. The role of conformational energies which defines the flexibility of polymer chains at thermodynamic equilibrium has to be included in the analysis. Having treated the glass transition as a cooperative transition in 1, we have obtained the relationships between the hole and flex energies and T_r. The present kinetic theory is an extension of the equilibrium analysis and takes into account the inter- and intramolecular interactions in a polymeric system.

On the basis of the idea of continuous conversion of the number of holes and the number of phonons in a polymer lattice, the hole energy is quantized for the purpose of describing the kinetics of free volume over the glass transition region. Because of the cooperative constraint, the multiple conformational energy states are also introduced to analyze the nonequilibrium behavior.

The departures from equilibrium for holes and bond rotations are treated as a non-Markovian process. The activation energies controlling the local relaxations are determined from the equilibrium (hole, flex) energies in Table I. When further analysis is carried out under the assumption of self-similarity, the distribution of the relaxation times for holes or rotamers can be described by a fractal exponent, β or γ, which also provides the important link between the global and local relaxation time scales.

The theoretical calculation reveals how the kinetics of holes and bond rotations affect the enthalpy relaxation. The conformational activation energy is found to be between 1 and 2 orders of magnitude lower than the hole activation energy. As a result, the conformational change occurs only in the initial stage of the annealing process. Because $v_f/\bar{v} \ll \epsilon_f/\epsilon_h \simeq {}^1/_2$, the dominant contribution to volume change is from holes. Under isothermal annealing followed by quenching, the theory predicts that the enthalpy relaxes much faster than volume at short times but approaches the same relaxation rate of volume at long times.

Acknowledgment. I thank W. M. Prest, Jr., and R. C. Penwell for several helpful discussions.

Appendix: $\langle \Delta r^2 \rangle$ versus λ_h

To include the spatial vector ($\vec{r}$) into the analysis, $h_i(t)$ is related to the hole concentration $C_i(r,t)$ by integrating over the volume surrounding an individual hole

$$h_i(t) = \int C_i(\vec{r},t) \, d\vec{r} \tag{A-1}$$

When the necessary condition of convergence is assumed, we rewrite eq 6 as[10]

$$\partial C_i(\vec{r},t)/\partial t = \sum_{m=1}^{\infty} (-\nabla)^m b_{im}(\vec{r}) C_i(\vec{r},t)/m! \tag{A-2}$$

where b_{im} in the mth moment of the transition rate $\Lambda_i(\vec{r}\,'|\vec{r})$ jumping from $\vec{r}$ to $\vec{r}\,'$:

$$b_{im} = \int (\vec{r}\,' - \vec{r})^m \, \Lambda_i(\vec{r}\,'|\vec{r}) \, d\vec{r}\,' \tag{A-3}$$

When an amorphous melt is quenched from the liquid state, a highly nonequilibrium state of hole concentration is created. Under the influence of such a concentration gradient against the spatial-dependent local energy barriers, the excited holes start to jump locally with a drift velocity b_{i1} which is considered as the dominant term on the right-hand side of eq A-2. In the time interval Δt, which is orders of magnitude longer than the jumping time, the displacement of a hole in the ith state can be written from eq A-2 as

$$\Delta r_i = \left| \int \Delta\vec{r} C_i \, d\vec{r} \right| = b_i \Delta t \tag{A-4}$$

where $b_i = |b_{i1}| = l/\tau_h^{(i)}\lambda_h$. Under the assumption of self-similarity (see p 118 of ref 14), the statistical average of displacements in different time intervals is independent

$$\langle \Delta r_j \Delta r_k \rangle = 0 \qquad \text{for } j \neq k \tag{A-5}$$

The mean square distance in the ith state is

$$\langle \Delta r_i^2 \rangle = K \langle (b_i \Delta t)^2 \rangle = t b_i^2 \langle \Delta t^2 \rangle / \Delta t \tag{A-6}$$

In this, the time interval (0, t) is divided into K equal segments and $K = t/\Delta t$ where t is much longer than Δt. Averaging over holes in all states and using eq A-6, we get

$$\langle \Delta r^2 \rangle = \frac{1}{n} \sum_{i=1}^{L} n_i \langle \Delta r_i^2 \rangle = t \overline{b^2} \langle \Delta t^2 \rangle / \Delta t \tag{A-7}$$

where $\overline{b^2} = \sum_i b_i^2 n_i / n \sim l^2/\lambda_h^2$. Thus, we have

$$\langle \Delta r^2 \rangle \sim 1/\lambda_h^2 \tag{A-8}$$

References and Notes

(1) *Ann. N.Y. Acad. Sci.* **1981**, *371*.
(2) *Polym. Eng. Sci.* **1984**, *24*(14).
(3) *J. Rheol.* **1986**, *30*(4).
(4) Struik, L. C. E. *Physical Aging in Amorphous Polymers and Other Materials*; Elsevier: Amsterdam, 1978.
(5) Hirai, H.; Eyring, H. *J. Polym. Sci.* **1959**, *37*, 51.
(6) Robertson, R. E. *J. Polym. Sci., Polym. Phys. Ed.* **1979**, *17*, 597.
(7) Curro, J. G.; Lagasse, R. R.; Simha, R. *Macromolecules* **1982**, *15*, 1621.
(8) Robertson, R. E.; Simha, R.; Curro, J. G. *Macromolecules* **1984**, *17*, 911.
(9) Cohen, M. H.; Grest, G. S. *Phys. Rev.* **1979**, *B20*, 1077.
(10) Chow, T. S. *J. Chem. Phys.* **1983**, *79*, 4602; *Macromolecules* **1984**, *17*, 2336.
(11) Chow, T. S. *Macromolecules* **1988**, preceding paper in this issue.
(12) Landau, L. D.; Lifshitz, E. M. *Statistical Physics*, 2nd ed.; Pergamon: Oxford, 1969; Chapters 5 and 6.
(13) Gibbs, J. H.; DiMarzio, E. A. *J. Chem. Phys.* **1958**, *28*, 373.
(14) Falconer, K. J. *The Geometry of Fractal Sets*; Cambridge University Press: Cambridge, 1985; Chapter 8.
(15) Mandelbrot, B. B. *The Fractal Geometry of Nature*; Freeman: New York, 1983.
(16) Chow, T. S. *J. Polym. Sci.* **1987**, *25B*, 137; *J. Rheol.* **1986**, *30*, 729.
(17) Chow, T. S. *Polymer* **1988**, *29*, 1447.

(18) Doolittle, A. K. *J. Appl. Phys.* **1951**, *22*, 1471.
(19) Koenig, J. L.; Antoon, M. K. *J. Polym. Sci., Polym. Phys. Ed.* **1977**, *15*, 1379.
(20) Prest, W. M., Jr.; Penwell, R. C. *Polym. Prepr. (Am. Chem. Soc., Div. Polym. Chem.)* **1980**, *21*, 10.
(21) Chow, T. S.; Prest, W. M., *Jr. J. Appl. Phys.* **1982**, *53*, 6568.
(22) Prest, W. M., Jr.; Roberts, F. J.; Kovacs, A. J. *Bull. Am. Phys. Soc.* **1984**, *29*(3), 326.
(23) Tribone, J. J.; O'Reilly, J. M.; Greener, J. *Macromolecules* **1986**, *19*, 1732.

^{13}C and ^{29}Si NMR Investigations of Glass-Filled Polymer Composites

T. L. Weeding and W. S. Veeman*

Department of Molecular Spectroscopy, Faculty of Science, University of Nijmegen, Toerhooiveld, 6525 ED Nijmegen, The Netherlands

L. W. Jenneskens, H. Angad Gaur, H. E. C. Schuurs, and W. G. B. Huysmans

AKZO Corporate Research Arnhem, P.O. Box 60, 6800 AB Arnhem, The Netherlands.

Received February 10, 1988; Revised Manuscript Received July 11, 1988

ABSTRACT: ^{13}C and ^{29}Si CP/MAS NMR have been employed to characterize the filler, the matrix, and the interfacial regions of microcomposite samples. As the interfacial region is the most important in determining the properties of a composite, we have focused our attention on this region with the goal of gaining insight into the adhesive mechanism on a molecular level. Five samples have been studied: the pure matrix polymer, the polymer plus the coupling agent only, the polymer plus the filler only, and two "complete" composites, one prepared from the polymer plus filler pretreated with the coupling agent and a second prepared by integral blending of the three components. The microcomposites were prepared with glass microspheres, polyamide-6, and the coupling agent (γ-aminopropyl)triethoxysilane. The spectra demonstrate differences between the interfacial layers of the composites that depend upon both the components which are present and upon the method of preparation.

Introduction

Composites are widely used as high-performance structural materials. Composites which consist of a particle or mineral-filled reinforced polymer matrix belong to the major class of microcomposites. The adhesion mechanism between the filler and matrix controls the transfer of stress and consequently strongly influences the final properties of the composites. Usually adhesion can be considerably enhanced by the addition of an appropriate bifunctional coupling agent such as a silane reagent (ca. 0.1–1% w/w). Various theories have been proposed to explain this phenomenon. One of these is the chemical bonding theory, which states that the formation of covalent chemical bonds between the coupling agent and the filler, and between the coupling agent and the matrix, leads to increased adhesive stability.[1] However, this theory has been unable to rationalize some of the properties of composites. An extension of the chemical bonding theory is the interpenetrating network (IPN) theory, which states that the matrix can diffuse into the coupling agent interphase to form an entangled network,[2] this also leads to increased adhesive stability. However, the adhesion mechanism has not yet been elucidated at the molecular level. Clearly a detailed knowledge of chemical and structural changes that occur in the composite, especially in the interphase region, is of interest for the optimization of composite properties. Solid-state NMR is ideally suited to this task since it allows one to nondestructively examine the environments of specific nuclei (^{29}Si and ^{13}C) in the matrix and on the surface of the filler, i.e., in the interfacial region. The purpose of this study is to explore the details of the adhesive mechanism which are manifest in the NMR spectra of composite samples.

We report here on a detailed investigation of microcomposites made of polyamide-6 (PA6), glass microspheres, and the coupling agent (γ-aminopropyl)triethoxysilane (γ-APS). Five samples were examined: pure PA6, PA6 plus γ-APS, PA6 plus glass microspheres, and two samples containing all three components. The three-component composites were prepared in two different ways: (a) pretreated glass microspheres were added to the PA6 and (b) the coupling agent was added to the glass microsphere–matrix mix in the melt in the "integral blending" process.

The chemistry involved in the preparation of the composites comprises many reactions. It is well established that the ethoxy groups of γ-APS hydrolyze[3] to give silanol groups which can then react further.

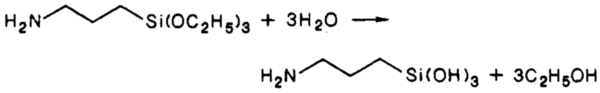

(1)

One of these reactions is the condensation reaction between molecules of hydrolyzed γ-APS to give a polysiloxane polymer.

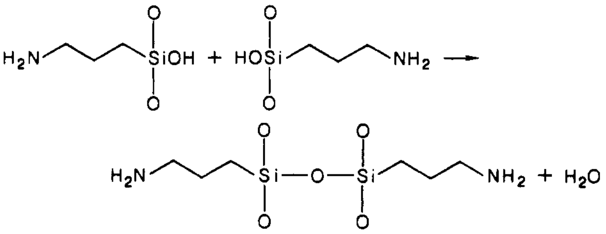

(2)

Reaction of the amine of γ-APS with the carboxylic end groups of PA6 gives an amide bond, the desired covalent linkage between the polymer and the coupling agent.

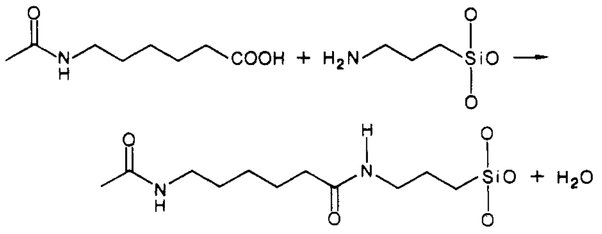

(3)

Covalent bonds between the surface of the glass micro-

0024-9297/89/2222-0706$01.50/0